Evaluation of peptide-aldehyde inhibitors using R188I mutant of SARS 3CL protease as a proteolysis-resistant mutant

Kenichi Akaji [a,*], Hiroyuki Konno [a], Mari Onozuka [a], Ayumi Makino [b], Hiroyuki Saito [b], Kazuto Nosaka [a]

[a] Department of Chemistry, Graduate School of Medical Science, Kyoto Prefectural University of Medicine, Kita-ku, Kyoto 603-8334, Japan
[b] Department of Biophysical Chemistry, Kobe Pharmaceutical University, Kobe 658-8558, Japan

ARTICLE INFO

ABSTRACT

The 3C-like (3CL) protease of the severe acute respiratory syndrome (SARS) coronavirus is a key enzyme for the virus maturation. We found for the first time that the mature SARS 3CL protease is subject to degradation at 188Arg/189Gln. Replacing Arg with Ile at position 188 rendered the protease resistant to proteolysis. The R188I mutant digested a conserved undecapeptide substrate with a K_m of 33.8 μM and k_{cat} of 4753 s^{-1}. Compared with the value reported for the mature protease containing a C-terminal His-tag, the relative activity of the mutant was nearly 10^6. Novel peptide-aldehyde derivatives containing a side-chain-protected C-terminal Gln efficiently inhibited the catalytic activity of the R188I mutant. The results indicated for the first time that the tetrapeptide sequence is enough for inhibitory activities of peptide-aldehyde derivatives.

1. Introduction

Severe acute respiratory syndrome (SARS), a life-threatening form of pneumonia, is caused by a new coronavirus (SARS CoV).[1–3] Although the primary SARS epidemic affecting about 8500 patients and leaving 800 dead was eventually controlled, no effective therapy exists for this viral infection. SARS CoV is a positive-sense, single-stranded RNA virus featuring the largest viral RNA genome known to date.[4,5] The genomic RNA produces two large proteins with overlapping sequences, polyproteins 1a (∼450 kDa) and 1ab (∼750 kDa), which are auto-catalytically cleaved by two or three viral proteases to yield functional polypeptides.[6] The key enzyme in this processing is a 33-kDa protease called 3C-like protease (3CL protease), because its substrate specificity is similar to that of the picornavirus 3C protease.[7,8] The SARS 3CL protease is a cysteine protease with a chymotrypsin fold, and cleaves precursor proteins at as many as 11 conserved sites involving a conserved Gln at the P1 position and a small amino acid (Ser, Ala, or Gly) at the P1' position with varying efficiency.[9,10] The 3CL protease exists as a homodimer and each 33-kDa protomer has its own active site containing a Cys-His catalytic dyad (Fig. 1A). Interactions between the C-terminal domain-III of each protomer play an important role in the formation of this dimer. The N-terminal end of one protomer is also expected to interact with the domain-II of another protomer to fold the dimeric structure. Although some studies reported that the addition of several residues to the C-terminus of mature 3CL protease did not significantly affect its activity, the kinetic properties and specificity of the mature protease have not been well described.

Due to its functional importance in the viral life cycle, the 3CL protease is considered an attractive target for the structure-based design of drugs against SARS.[11–17] Several crystal structures of the SARS 3CL protease with or without inhibitors have also been used to evaluate various types of inhibitors for this protease.[8,18–21] Most inhibitors contain a functional group such as a chloromethyl ketone, Michael acceptor, or epoxide that can react irreversibly with the active-site cysteine residue. Few studies regarding reversible inhibitors containing an aldehyde group as a functional group have been reported.[22] In the course of our own studies on the SARS 3CL protease and its inhibitors, we found that the mature protease could be further processed into two fragments devoid of catalytic activity. Here, we report on high level of expression in *Escherichia coli* and the purification of a proteolysis-resistant mutant of the SARS 3CL protease. The kinetic characterization of this mutant revealed remarkable potency compared with the mature 3CL protease containing a C-terminal His-tag. The potency makes it possible to evaluate newly synthesized peptide-aldehyde inhibitors quantitatively by conventional HPLC.

2. Results and discussion

2.1. Expression of the mature 3CL protease

We first intended to obtain the mature 3CL protease from a fusion protein containing maltose-binding protein (MBP), His$_6$ and a

A. mature SARS 3CL protease

```
        10         20         30         40         50
SGFRKMAFPS GKVEGCMVQV TCGTTTLNGL WLDDTVYCPR HVICTAEDML

        60         70         80         90        100
NPNYEDLLIR KSNHSFLVQA GNVQLRVIGH SMQNCLLRLK VDTSNPKTPK

       110        120        130        140        150
YKFVRIQPGQ TFSVLACYNG SPSGVYQCAM RPNHTIKGSF LNGSCGSVGF

       160        170        180        190        200
NIDYDCVSFC YMHHMELPTG VHAGTDLEGK FYGPFVDRQT AQAAGTDTTI

       210        220        230        240        250
TLNVLAWLYA AVINGDRWFL NRFTTTLNDF NLVAMKYNYE PLTQDHVDIL

       260        270        280        290        300
GPLSAQTGIA VLDMCAALKE LLQNGMNGRT ILGSTILEDE FTPFDVVRQC

       306
SGVTFQ
```

B. Fusion protein containing SARS 3CL protease
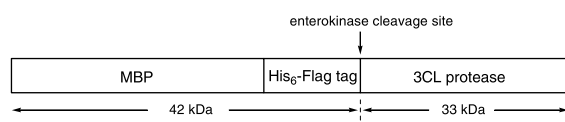
Figure 1. (A) Amino acid sequence of SARS CoV 3CL protease: the catalytic dyad is defined by His 41 and Cys 145, which is similar to the arrangement found in other coronavirus proteases. The N-terminal part (1–184, Domain I and II) is composed of a two-β-barrel fold similar to that of a chymotrypsin-type protease. The C-terminal part (201–303, Domain-III) has five α-helices. (B) Fusion protein composed of MBP, His6 and a Flag-tag, and 3CL protease.

Flag-tag, and mature 3CL protease (MBP-His tag-3CL protease, Fig. 1B). The corresponding plasmid was introduced into *E. coli*, and the desired fusion protein of 75-kDa was obtained as a major product of the total cell lysate (Fig. 2A, lane 1). The fusion protein was easily purified with a cobalt affinity column to give a single major band on SDS–PAGE (Fig. 2A, lane 2). The 75-kDa product did not cleave SO1, an undecapeptide substrate (H-Thr-Ser-Ala-Val-Leu-Gln-Ser-Gly-Phe-Arg-Lys-NH2) containing the P1/P2 cleavage site of 3CL protease, probably because of an N-terminal fused large protein. After digestion of the fusion protein with enterokinase, the N-terminal 42-kDa fragment containing the MBP was de-

tected, but the desired 33-kDa protein corresponding to the mature 3CL protease was hardly detected (Fig. 2A, lane 3). To confirm whether the 33-kDa protein was produced or not, we then added enterokinase in the presence of a protease substrate; the substrate SO1 was mixed with the fusion protein prior to the addition of the enterokinase. In this reaction mixture, the substrate completely disappeared within 1 h, and expected fragment peptides were clearly identified by MALDI-TOF-MS (Fig. 2B; peak 1, [M+H]+ 593.365 (Calcd. 593.353) for H-Ser-Gly-Phe-Arg-Lys-NH2; peak 2, [M+H]+ 618.288 (Calcd. 618.347) for H-Thr-Ser-Ala-Val-Leu-Gln-OH). This result suggests that the mature 3CL protease was temporarily produced by the digestion of the 75-kDa fusion protein by the enterokinase.

We then tried to directly express the 3CL protease containing a C-terminal His-tag as described previously.[9] The necessary plasmid was constructed from the previous plasmid, and introduced into *E. coli*. The desired 34-kDa product containing the mature 3CL protease was not detected as a major product (Fig. 2C, lane 1) in our experiment. After purification with a cobalt column, a small amount of 34-kDa product was detected by Coomassie staining and Western blotting using anti-His-tag antibody (Fig. 2C, lane 2, Fig. 2D, lane 1). The immunostaining, however, decreased in intensity gradually and a 14-kDa protein emerged after placement at room temperature (Fig. 2D, lane 2), or overnight incubation with enterokinase (Fig. 2D, lane 3). These results strongly suggest that mature 3CL protease is susceptible to degradation by proteolysis.

To identify the probable cleavage site, enterokinase-based digestion of the 75-kDa fusion protein, MBP-His tag-3CL protease (Fig. 3, lane 1), was carefully examined. After 15 min of treatment with a small amount of enterokinase, the desired 33-kDa product was detected as a faint band by Coomassie staining. Two additional bands at 20- and 13-kDa were also detected (Fig. 3, lane 2) as probable products of the proteolysis. The faint band of 33-kDa disappeared with prolonged treatment over 60 min (Fig. 3, lanes 3–4). The newly emerged 13-kDa protein seemed to be the same product obtained from the C-terminal His-tagged 3CL protease (Fig. 2D, lanes 2–3). By blotting the 13-kDa protein to a polyvinylidene difluoride(PVDF), the N-terminal sequence of the product was determined to be Gln-Thr-Ala-Gln-Ala, which shows that mature 3CL protease is cleaved at the 188Arg/189Gln site.
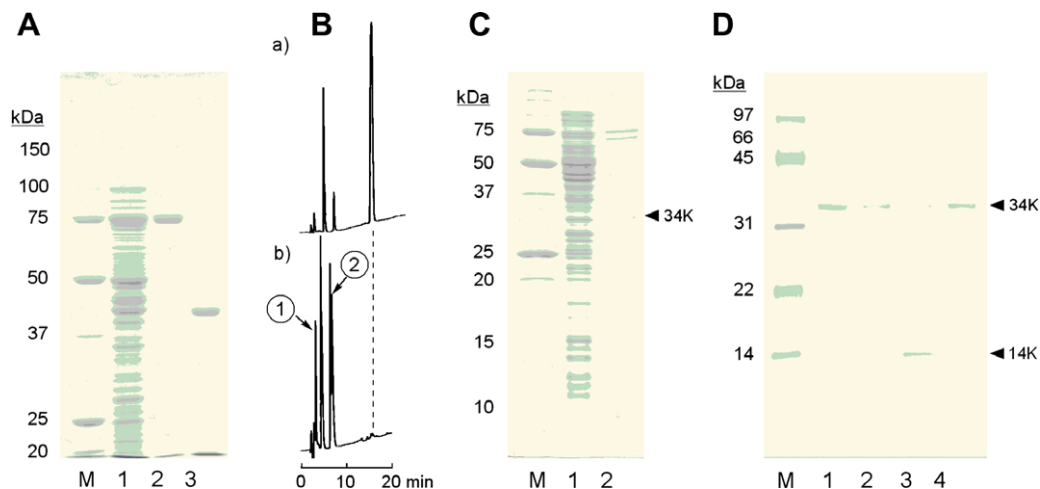
Figure 2. Expression of mature 3CL protease: (A) SDS–PAGE (10%) of MBP-His-Flag-tagged 3CL protease stained with Coomassie brilliant blue; lane M, molecular standard proteins (Bio-Rad); lane 1, crude extract (20 μg of protein) of IPTG-induced bacterial cells; lane 2, metal affinity resin-treated fraction (3 μg); lane 3, enterokinase-treated (0.1 U for 2 h) fraction (3 μg). (B) (a) HPLC profile of the substrate SO1 in the reaction buffer, (b) HPLC profile of the mixture of 75-kDa fusion protein, enterokinase, and SO1 after 4 h of treatment. Peak 1 derives from the C-terminal cleavage fragment of SO1 and peak 2 derives from the N-terminal cleavage fragment. (C) SDS–PAGE (15%) of C-terminal His-tagged 3CL protease stained with Coomassie brilliant blue; lane M, molecular standard proteins (Bio-Rad); lane 1, crude extract (20 μg of protein) of IPTG-induced bacterial cells; lane 2, metal affinity resin-treated fraction (4 μg). (D) Western blotting of C-terminal His-tagged 3CL protease using anti-His-tag antibody; lane M, molecular standard proteins (Bio-Rad); lane 1, metal affinity resin-treated fraction (4 μg); lane 2, after overnight incubation at room temperature; lane 3, after incubation with enterokinase (0.05 U); lane 4, after incubation with purified 3CL-R188I protease (0.5 μg).
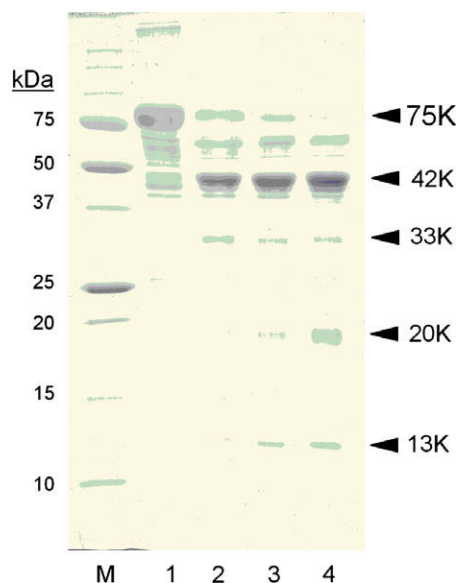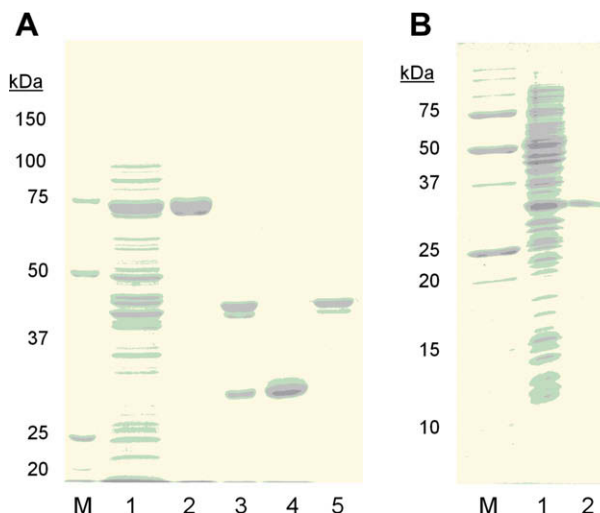
Figure 3. Time course of enterokinase (0.05 U)-based digestion of the metal affinity resin-treated fusion protein containing the mature 3CL protease (10 μg): lane 1, untreated; lane 2, 15 min; lane 3, 30 min; lane 4, 60 min.

Figure 4. SDS–PAGE of R188I mutant 3CL protease: samples at each purification step were separated by 10% (A) or 15% (B) SDS–PAGE and stained with Coomassie brilliant blue. Lanes M indicate molecular standard proteins (Bio-Rad). (A) Untagged protease: lane 1, crude extract (20 μg of protein) of bacterial cells expressing the N-terminal MBP-His-Flag-tagged protease; lane 2, metal affinity resin-treated fraction (6 μg); lane 3, enterokinase-treated fraction (4 μg); lane 4, DEAE–Sepharose column flow-through fraction (3 μg); lane 5, DEAE–Sepharose column-retained fraction (3 μg). (B) C-terminal His-tagged protease: lane 1, crude extract (20 μg of protein) of IPTG-induced bacterial cells; lane 2, metal affinity resin-treated fraction (2 μg).

The 188Arg/189Gln site is in a long loop region (residue 185–200) which connects a chymotrypsin-like catalytic domain I–II (1–184) and C-terminal α-helical domain-III (201–303) of mature 3CL protease (Fig. 1). In a homodimeric structure of mature 3CL protease, the α-helical domain is expected to be responsible for orienting the amino terminus of one monomer to a position in which it can interact with the active site of the other monomer.[23] It was also reported that the expression of the N-terminal catalytic region alone yields a protein with reduced catalytic efficiency.[18] Thus, the expected biological role of the α-helical domain is consistent with our finding that proteolysis at the 188Arg/189Gln site rapidly reduces the catalytic efficiency of mature 3CL protease.

2.2. Expression and characterization of R188I mutant 3CL protease

To obtain an active and stable 3CL protease, we then constructed a mutant in which Arg-188 was substituted with Ile (3CL-R188I) by site-directed mutagenesis. This substitution was selected to remove the ionic guanidine group without remarkably changing the steric effect of the Arg side-chain. Similar to wild-type 3CL protease, 3CL-R188I protease was expressed in *E. coli* as a fusion protein, MBP-His-tag-R188I mutant. The 75-kDa fusion protein was obtained as a major product, and easily purified with metal affinity resin (Fig. 4A, lanes 1 and 2). After enterokinase treatment, the desired 33-kDa product corresponding to 3CL-R188I protease was intensely stained with Coomassie, and no proteolytic product was detected (Fig. 4A, lane 3). The 3CL-R188I protease was further purified by anion exchange chromatography at pH 5.5: the R188I protease with a calculated p*I* of 6.24 flowed through and the MBP-His$_6$-Flag of p*I* 5.08 was absorbed on the resin as expected (Fig 4A, lanes 4 and 5). About 0.10 mg of the purified untagged protein was obtained from 100 ml of bacterial culture. A 34-kDa protein corresponding to 3CL-R188I with the C-terminal His tag was also directly produced as a major product (Fig. 4B, lane 1). A single step of purification with metal affinity resin was enough to obtain a highly purified product (Fig. 4B, lane 2). In this case, about 0.13 mg of the purified C-terminal His-tagged protein was obtained from 100 ml of culture. These purified mutant proteins with or without a C-terminal

His tag were concentrated by ultrafiltration, and an equal volume of glycerol was added. Each solution was stored at −20 °C without any loss of catalytic activity for at least a year.

The catalytic activities of purified 3CL-R188I proteases were examined using three different substrates (SO1, SO3, and SR1). SO1 containing the P$_1$/P$_2$ cleavage site, the N-terminal self-cleavage site of the protease, is reported to be the most suitable substrate, a canonical substrate, for 3CL protease.[9] SO3 is an undecapeptide containing the non-canonical P$_3$/P$_4$ cleavage site of 3CL protease, and SR1 is a hexadecapeptide containing a newly found proteolytic site (188Arg/189Gln). Each substrate, at different concentrations, was incubated with the mutant protease at 37 °C, and the cleavage reaction was monitored with analytical HPLC as in Fig. 2B. The initial digestion rate was calculated from the decrease in the initial amount of substrate, and each kinetic parameter was calculated by plotting [S]/*v* against [S].

As summarized in Table 1, the catalytic ability of 3CL-R188I protease was found to be extreme as compared to that of a previously reported mature 3CL protease containing a C-terminal His tag[9], especially the k_{cat} values; 12.2 min^{-1} for mature 3CL protease and 4753 s^{-1} for the 3CL-R188I. The activity of the mutant relative to the mature protease was nearly 10^6. Addition of a C-terminal His-tag lowered the relative activity to 0.03 owing to a significant decrease in the k_{cat} value. The results suggest that the additional sequences at the N- and C-terminus of mature 3CL protease remarkably affect the catalytic activities even with several additions as expected from the maturation analysis.[24]

Table 1
Catalytic parameters and relative efficiency of the SARS 3CL R188I mutant protease for three different peptides

Tag of protease	Substrate	K_m (μM)	k_{cat} (s^{-1})	k_{cat}/K_m (μM s^{-1})	Relative rate
None	SO1	33.8	4753	156.9	1.00
C-terminal His tag	SO1	31.8	153	4.8	0.03
None	SO3	50.5	455	9.1	0.06
None	SR1	46.0	76	2.0	0.01

The relative efficiency for SO3 and SR1 was 0.06 and 0.01, respectively, when compared with the k_{cat}/K_m for SO1. The relative efficiency for SO3 vs. SO1 was exactly the same as reported for the mature protease.[9] The relative efficiency for SR1 was nearly the same as that reported for cleavage at the P_5/P_6 site, another non-canonical cleavage site of mature 3CL protease.[9] This suggests that mature 3CL protease can digest the precursor protein of SARS CoV at the Arg188/Gln189 site as at non-canonical cleavage sites. Thus, we examined the cleavage of mature 3CL protease by the mutant. Incubation of the C-terminal His-tagged mature 3CL protease with the purified 3CL-R188I protease gave the degradation product derived from the 3CL protease (Fig. 2D, lane 4). From these results, we suppose that 3CL protease can digest itself. Application of the mutant protease of the same size as the mature 3CL protease would be effective to accelerate the development of efficient inhibitors for the SARS CoV 3CL protease.

2.3. Peptide-aldehyde inhibitors

As a suitable candidate for a reversible-inhibitor, we selected a peptide-aldehyde containing the SO1 sequence. To obtain highly homogeneous derivatives efficiently, we constructed the aldehyde group by reduction of the corresponding Weinreb amide[25] prepared by solution phase synthesis. Thus, starting from Fmoc-Gln(Trt)-N(OMe)Me, peptide chain elongation was conducted using a combination of Fmoc-deprotection with diethylamine and a coupling reaction using BOP. The resulting peptapeptide Weinreb amide, Ac-Ser(OBu^t)-Ala-Val-Leu-Gln(Trt)-N(OMe)Me, was then reduced with LiAlH$_4$ and the remaining side-chain protecting groups were removed with TFA (Scheme 1). The deprotected product was purified by HPLC to yield a product showing a single peak. A ^{1}H NMR spectrum of the product, however, gave no aldehyde signal, but showed an additional methyl signal at 2.57 ppm. MALDI-TOF-MS also showed a higher molecular weight than expected. These spectral data strongly suggest that the reduction with lithium aluminum hydride did not proceed as expected. The LiAlH$_4$ attacked the methoxy group instead of the carbonyl carbon probably because of the large steric hindrance of the Trt group at the C-terminal Gln side chain, and gave a corresponding methyl-amide derivative (Scheme 1).
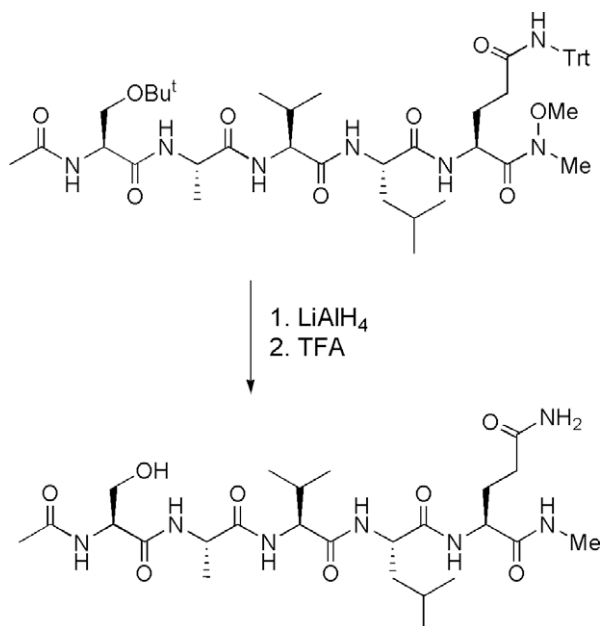
To avoid this undesired reaction, we then synthesized the peptide-aldehyde using the Gln(Me$_2$) derivative. Use of the side-chain-protected Gln is also effective at preventing equilibrium between the desired C-terminal aldehyde and the corresponding hemiaminal formed with an unprotected amide at the Gln side-chain.[26] Starting from Fmoc-Glu-OBu^t, dimethylamine was condensed to the side-chain carboxyl group. Then, the α-*tert*-butyl ester was cleaved and converted to the Weinreb amide. Subsequent peptide chain elongation was conducted as before using a combination of Fmoc-deprotection with diethylamine and coupling with BOP (Scheme 2). The resulting hexapeptide amide was then reduced with LiAlH$_4$. After deprotection with TFA, the crude product was purified by HPLC to give a single peak on analytical HPLC. MALDI-TOF-MS and NMR analyses gave results confirming the aldehyde structure. Peptide aldehydes containing truncated chains were similarly synthesized from the corresponding intermediates and purified.

The inhibitory effects of newly synthesized peptide-aldehyde inhibitors were assayed using the purified untagged 3CL-R188I protease. The substrate peptide SO1 was incubated with the mutant protease in the presence of various concentrations of peptide-aldehyde, and the reaction mixture was analyzed by HPLC as in Fig. 2B. From the decrease in SO1 at the respective concentration of inhibitor, a sigmoidal dose-response curve was obtained (Fig. 5), and each IC$_{50}$ value was estimated from each sigmoid curve. As summarized in Table 2, the tetrapeptide sequence was long enough for inhibitory activity. The activity increased in parallel with chain length; the hexapeptide aldehyde had an IC$_{50}$ of 26 μM. E-64[27], a typical cysteine protease inhibitor, showed nearly the same inhibitory activity (36% inhibition at 5.6 mM) as Ac-Val-Leu-Gln(Me$_2$)-CHO, which suggests that the peptide-aldehyde derivatives would be a promising reversible SARS 3CL protease inhibitor. Detailed structure–activity studies are now underway.

3. Experimental

The pMAL-c2X-based (NEB BioLabs) bacterial expression vector, pMAL-3CL, was kindly provided by Dr. Norio Yamamoto and Prof. Naoki Yamamoto (Tokyo Medical and Dental University). pMAL-3CL encodes a 75-kDa protein containing a full-length SARS CoV 3CL protease with a maltose-binding protein, a six-histidine tag, and a Flag tag (MBP-His-Flag) at the N-terminus, and is designed to release mature 3CL protease with a free N-terminus from the fusion protein on enterokinase treatment.

E-64 was purchased from Peptide Institute, Inc. (Osaka, Minoh, Japan). Fmoc amino acid derivatives were purchased form Watanabe Chemical, Inc. (Hiroshima, Japan). Analytical and preparative HPLCs were performed using a HITACHI ELITE LaChrom system (OD, 220 nm) equipped with the Nacalai tesque COSMOSIL 5C18-AR-II (4.6×150 mm or 10×250 mm) reversed phase column. The product was eluted with a gradient of CH$_3$CN containing 0.1% TFA in 0.1% aqueous TFA solution. ^{1}H (300 MHz) and ^{13}C (75 MHz) NMR spectra were recorded on a Bruker AM-300. Chemical shifts are expressed in parts per million relative to TMS (0 ppm) or CHCl$_3$ (7.28 ppm for ^{1}H and 77.0 ppm for ^{13}C). High resolution MALDI TOF-MS mass spectra were obtained on a Bruker Autoflex-II. Optical rotations were recorded on a HORIBA SEPA-300 polarimeter at the sodium D line.

3.1. Expression of mature 3CL proteases

The full-length 3CL protease-coding sequence was amplified from pMAL-3CL with 5′-ccggctagcGGTTTTAGGAAAATGGCATTCC containing a NheI site and 5′-ccgctcgagTTGGAAGGTAACACCAGAG containing a XhoI site. The PCR product was cloned directly into pGEM T-easy (Promega) to produce pGEM-3CL. Another expression
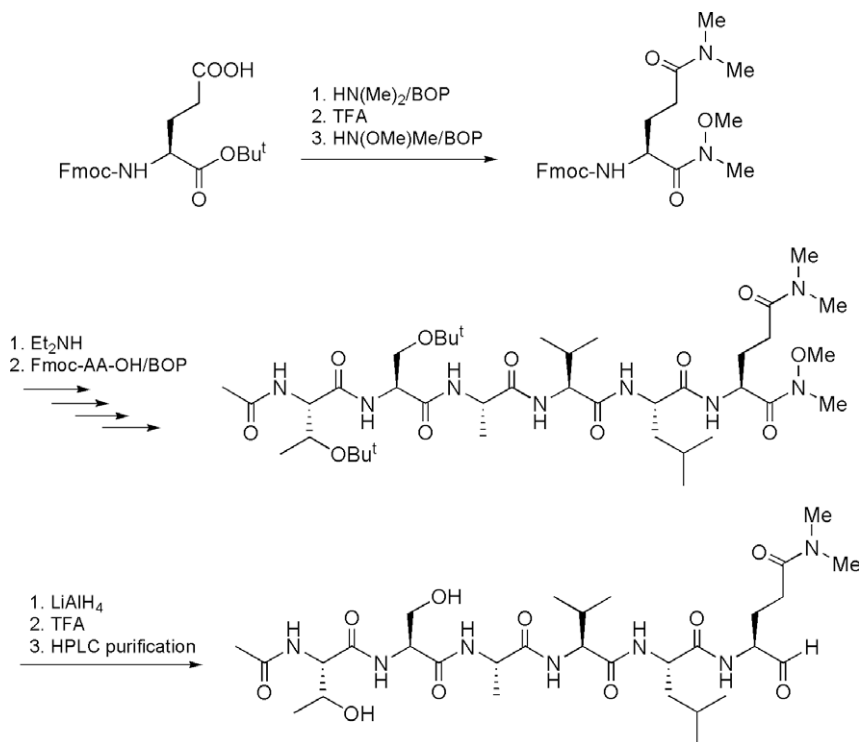
Scheme 1.

Scheme 2.
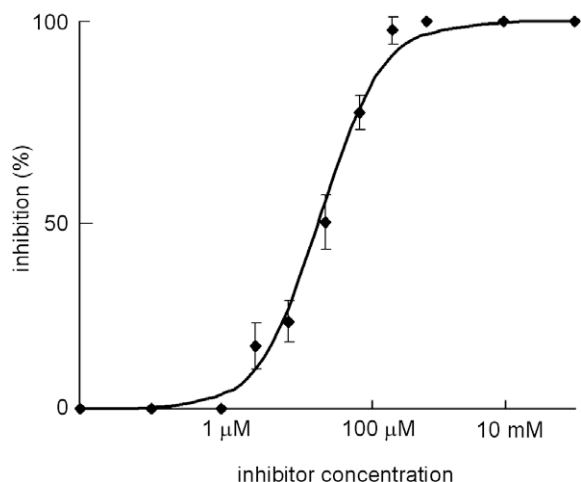
Figure 5. A typical sigmoidal dose–response curve used for estimation of the IC_{50} value of Ac-Thr-Ser-Ala-Val-Leu-NHCH(CH$_2$CH$_2$CON(CH$_3$)$_2$)-CHO.

Table 2
Inhibitory activities of peptide-aldehydes for SARS 3CL R188I mutant protease

Peptide aldehyde	IC_{50}
Ac-Val-Leu-NHCH(CH$_2$CH$_2$CON(CH$_3$)$_2$)-CHO	~ 6 mM
Ac-Ala-Val-Leu-NHCH(CH$_2$CH$_2$CON(CH$_3$)$_2$)-CHO	155 μM
Ac-Ser-Ala-Val-Leu-NHCH(CH$_2$CH$_2$CON(CH$_3$)$_2$)-CHO	37 μM
Ac-Thr-Ser-Ala-Val-Leu-NHCH(CH$_2$CH$_2$CON(CH$_3$)$_2$)-CHO	26 μM

vector, pET-3CL, was made by inserting the NheI–XhoI fragment corresponding to the 3CL protease-coding fragment of pGEM-3CL into the NheI/XhoI site of pET-21a(+) (Novagen), and encodes a 34-kDa protein containing a full-length 3CL protease with three N-terminal amino acids (Met-Ala-Ser) and two C-terminal amino acids (Leu-Glu) plus a His tag.

The pMAL-c2X-based plasmid and pET-21a(+)-based plasmid were transformed into *E. coli* strains DH5α and BL21(DE3)pLys, respectively. Bacterial cells were grown overnight at 37 °C in 10 ml of LB medium containing 50 μg/ml ampicillin, pelleted, and grown for 2 h in 100 ml of fresh medium. The cells were further shaken at 28 °C for 2 h with 0.5 mM isopropyl-β-D-thiogalactopyranoside (IPTG) to produce the recombinant protein. The cells were then pelleted and resuspended in 20 ml of solution L (50 mM Na$_2$HPO$_4$ pH 7.0, and 300 mM NaCl) containing 10 mM imidazole, 1 mM phenylmethylsulfonyl fluoride and 10 μl/ml of Protease Inhibitors Cocktail for purification of Histidine-Tagged Proteins (Sigma), and sonicated 4 times in ice-cold water using a Bioruptor (Cosmo Bio, Tokyo, Japan) at 200 W for 30 s each time with a 120-s interval. Cell debris was removed by centrifugation at 14,000g for 20 min, and the supernatant served as a crude extract. The crude extract was applied to a 1 ml bed volume of TALON Metal Affinity Resin (Clontech) equilibrated with solution L containing 10 mM imidazole. After being washed with 20 ml of the same solution, the protease was eluted with solution L containing 125 mM imidazole. Combined eluted fractions (1.3 ml) were concentrated to 0.2 ml during exchange of the buffer with 20 mM Tris–HCl pH 7.5 by ultrafiltration using Centricon YM-10 (10 kDa cutoff, Millipore).

3.2. Identification of degradation products from mature 3CL-protease

The affinity resin-purified fraction (12 μg protein) of the N-terminal MBP-His-Flag-tagged 3CL protease was incubated with 1 U of enterokinase for 30 min at 21 °C, and then separated on 15% SDS–PAGE gels and transferred to a PVDF membrane. After Coomassie blue staining, the 20- and 13-kDa bands were dissected and subjected to Edman sequencing for determination of the N-terminal.[28] This analysis was performed using an Applied Biosystems 491 Protein Sequencer at APRO Life Science Institute (Naruto, Japan).

3.3. Expression of 3CL-R188I mutant proteases

Site-directed mutagenesis was performed by the inverse PCR method described by Stemmer and Morris.[29] The primers used to generate point mutations were 5′-atctctCGTCTCCA*T*ACAAACTGCAC AGGCTG (nucleotide in italics is mutated) and 5′-atctctCGTCTCTGT*A* TGTCAACAAATGGACC, and PCR was performed with the plasmid pGEM-3CL as the template. After PCR, the ends of the full-length linearized plasmids were digested with BsmBI (CGTCTCN'NNNN), leaving plasmids with compatible overhangs at both ends. Expression vectors pMAL-3CL-R188I and pET-3CL-R188I were constructed by replacing the short SphI–StyI fragment of pMAL-3CL and the short NheI–XhoI fragment of pET-3CL with the corresponding fragments of pGEM-3CL-R188I, respectively. Sequencing was carried out to confirm the presence of only the desired mutation and no unintentional changes.

For purification of the untagged 3CL-R188 L protease, the metal affinity resin-treated fraction of the N-terminal MBP-His-Flag-tagged protease (about 1.5 mg protein) was further incubated with 17 U of recombinant enterokinase (Novagen) for 2 h at 21 °C in 1 ml of a buffer containing 20 mM Tris–HCl pH 7.4, 50 mM NaCl, and 2 mM CaCl$_2$. After the enterokinase was removed from the solution using EKapture Agarose (Novagen), the buffer was changed to 20 mM Bis–Tris pH 5.5 using a Centricon YM-10. The enterokinase treated fraction was then applied to a 1 ml bed volume of DEAE Sepharose (GE Healthcare) equilibrated with the same buffer. The target protease flowed though the Sepharose resin and the MBP-His-Flag fragment was retained in the resin. Optionally, the bound protein could be eluted with the same buffer containing 0.5 M KCl.

The metal affinity resin-treated fraction of the C-terminal His-tagged 3CL protease was used as the substrate to examine degradation. After incubating the fraction (about 4 μg protein) for 14 h at room temperature with 0.05 U of enterokinase or with 0.5 μg of purified 3CL-R188L protease, the solution was separated on 15% SDS–PAGE gels and electroblotted onto a PVDF membrane. The His-tagged protease and its cleaved product were visualized using an anti-His-Tag monoclonal antibody (Novagen), a biotinylated anti-mouse IgG (Vector), and an amplified alkaline phosphatase Immun-Blot assay kit (Bio-Rad).

3.4. Substrate peptides

The substrate peptides (SO1; H-Thr-Ser-Ala-Val-Leu-Gln-Ser-Gly-Phe-Arg-Lys-NH$_2$: SO3; H-Lys-Val-Ala-Thr-Val-Gln-Ser-Lys-Met-Ser-Asp-NH$_2$: and SR1; H-Gly-Pro-Phe-Val-Asp-Arg-Gln-Thr-Ala-Gln-Ala-Ala-Gly-Thr-Asp-Thr-NH$_2$) were synthesized using Fmoc-based solid-phase peptide synthesis (SPPS)[30] starting with Rink amide resin (4-(2′,4′-dimethoxyphenyl-Fmoc aminomethyl)phenoxy resin).[31] SPPS was achieved by a combination of Fmoc deprotection using 20% piperidine/DMF and a coupling reaction using a standard diisopropylcarbodiimide/HOBt protocol. Each peptide was purified by preparative HPLC after cleavage from the resin by treatment with TFA thioanisole (10:1) at 25 °C for 3 h. Homogeneity was further confirmed by MALDI-TOF-MS. SO1; HPLC [Cosmosil 5C18 AR column (4.6 × 150 mm), 1.0 ml/min, CH$_3$CN (10–20%)/30 min] rt 19.62 min, m/z 1192.714 for [M+H]$^+$ (calcd 1192.681 for C$_{52}$H$_{90}$N$_{17}$O$_{15}$). SO3; HPLC [Cosmosil 5C18 AR column (4.6 × 150 mm), 1.0 ml/min, CH$_3$CN (10–20%)/30 min] rt 8.58 min, m/z 1192.288 for [M+H]$^+$ (calcd 1192.637 for C$_{49}$H$_{90}$N$_{15}$O$_{17}$S). SR1; HPLC [Cosmosil 5C18 AR column (4.6 × 150 mm), 1.0 ml/min, CH$_3$CN (10–50%)/30 min] rt 11.07 min, m/z 1633.758 for [M+H]$^+$ (calcd 1633.794 for C$_{68}$H$_{109}$N$_{22}$O$_{25}$).

3.5. Enzymatic activity

The proteolytic activities of 3CL proteases were detected by a cleavage assay of SO1 using analytical HPLC. Each peptide in

20 mM Tris–HCl buffer pH 7.5 containing 7 mM DTT was incubated with the protease at 37 °C and the cleavage reaction was monitored by analytical HPLC [Cosmosil 5C18 (4.6 × 150 mm), 1.0 ml/min, CH$_3$CN (10–20%)/30 min]. Each product of hydrolysis was identified by MALDI-TOF MS.

Kinetic parameters, K_m and k_{cat}, were determined by initial rate measurements of the hydrolysis of each substrate at 37 °C. Each reaction was initiated by adding the protease to various solutions containing different final concentrations of the substrate (0 to 168 μM). The final concentration of the enzyme (10 to 170 nM for the mutant protease) and the digestion time (15 to 90 min) varied because the cleavage activity differed for each substrate. After the reaction, aliquots were analyzed by HPLC. The initial digestion rates were calculated from the decrease in the peak area of each substrate. K_m was calculated from the plot of $[S]/v$ vs. $[S]$, where $[S]$ is the concentration of the substrate and v is the initial reaction rate. All reactions were repeated three times and the results were averaged.

3.6. Inhibitors

3.6.1. Fmoc-Gln(Me)$_2$-N(OMe)Me

HN(Me)$_2$. HCl salt (0.29 g, 3.56 mmol), BOP (1.59 g, 3.56 mmol), and DIEA (1.91 ml, 12 mmol) were added to Fmoc-Glu-OBu^t (1.28 g, 3 mmol) in CH$_2$Cl$_2$ (10 ml), and the mixture was stirred at 25 °C for 2 h. The solvent was evaporated and the residue was dissolved in AcOEt. The organic phase was washed with 5% citric acid, 5% NaHCO$_3$, and brine, and then dried over MgSO$_4$. The solvent was evaporated and the residue was purified by silica-gel column chromatography using CHCl$_3$:MeOH = 10:0.5. The desired product, without further purification, was treated with TFA (7.0 ml) in the presence of anisole (0.65 ml, 6.0 mmol). After stirring at 25 °C for 1 h, the TFA was evaporated at 25 °C. The residue was washed with hexane, and dried in vacuo. The residue was dissolved in DMF (10 ml), and HN(OMe)Me HCl salt (0.38 g, 3.90 mmol), BOP (1.72 g, 3.90 mmol), and DIEA (1.70 ml, 11 mmol) were added. The mixture was stirred at 25 °C for 8 h, and the solvent was evaporated. The residue was dissolved in AcOEt, and the organic phase was washed with 5% citric acid, 5% NaHCO$_3$, and brine, and then dried over MgSO$_4$. The solvent was evaporated and the residue was purified by silica-gel column chromatography using CHCl$_3$:MeOH = 10:0.5 to yield the desired product as an oil. Yield 1.13 g (85%), $[\alpha]_D^{27}$ +46.7 (c 0.24, CHCl$_3$), ^{1}H NMR (CDCl$_3$) δ; 2.00 (m, 1H), 2.16 (m, 1H), 2.42 (m, 2H), 2.94 (s, 3H), 2.95 (s, 3H), 3.22 (s, 3H), 3.79 (s, 3H), 4.22 (t, J = 7.1 Hz, 1H), 4.35 (m, 2H), 4.76 (br s, 1H), 5.91 (d, J = 8.1 Hz, 1H), 7.31 (d, J = 7.5 Hz, 2H), 7.39 (t, J = 7.5 Hz, 2H), 7.61 (br t, J = 8.3 Hz, 2H), 7.75 (d, J = 8.3 Hz, 2H); ^{13}C NMR δ; 27.72, 29.13, 32.29, 35.63, 37.24, 47.27, 51.04, 61.72, 67.09, 120.05, 125.23, 125.34, 127.15, 127.78, 141.37, 141.40, 143.89, 144.12, 156.39, 162.44, 171.99; MALDI-TOF-MS; Calcd. 462.201 for C$_{24}$H$_{29}$N$_3$O$_5$Na, Found. 462.126 for [M+Na]$^+$.

3.6.2. Fmoc-Leu-Gln(Me)$_2$-N(OMe)Me

Et$_2$NH (8.6 ml) was added to Fmoc-Gln-N(OMe)Me (0.73 g, 1.66 mmol) in CH$_3$CN (8 ml), and the mixture was stirred at 25 °C for 40 min. The solvent was evaporated and the residue was dried in vacuo. The residue was dissolved in CH$_2$Cl$_2$ (5 ml). Fmoc-Leu-OH (0.49 g, 1.39 mmol), BOP (0.61 g, 1.39 mmol), and DIEA (0.44 ml, 2.77 mmol) were added to the solution and the mixture was stirred at 25 °C for 8 h. The solvent was evaporated, and the residue was dissolved in AcOEt. The organic phase was washed with 5% citric acid, 5% NaHCO$_3$, and brine, and then dried over MgSO$_4$. The solvent was evaporated and the residue was purified by silica-gel column chromatography using CHCl$_3$:MeOH = 10:0.5 to yield the desired product as an oil. Yield 0.60 g (91%), $[\alpha]_D^{27}$ −27.6 (c 1.1,

CHCl$_3$), ^{1}H NMR (CDCl$_3$) δ; 0.94 (s, 3H), 0.96 (s, 3H), 1.53–1.63 (m, 2H), 1.66–1.72 (m, 1H), 2.00 (br s, 1H), 2.14–2.21 (m, 1H), 2.88 (s, 3H), 2.90 (s, 3H), 3.21 (s, 3H), 3.79 (s, 3H), 4.19–4.24 (m, 1H), 4.22 (d, J = 6.9 Hz, 1H), 4.29–4.42 (m, 2H), 4.92 (br s, 1H), 5.40 (d, J = 8.4 Hz, 1H), 7.32 (t, J = 7.5 Hz, 2H), 7.39 (t, J = 7.5 Hz, 2H), 7.59 (d, J = 7.5 Hz, 2H), 7.75 (d, J = 7.5 Hz, 2H); ^{13}C NMR δ; 22.06, 23.12, 24.77, 26.77, 29.18, 32.33, 35.70, 37.20, 42.19, 47.32, 49.64, 53.66, 61.71, 67.09, 120.06, 120.08, 125.22, 127.20, 127.82, 141.40, 143.97, 144.02, 156.19, 171.80, 172.36, 172.43; MALDI-TOF-MS; Calcd. 575.285 for C$_{30}$H$_{40}$N$_4$O$_6$Na, Found. 575.174 for [M+Na]$^+$.

3.6.3. Fmoc-Val-Leu-Gln(Me)$_2$-N(OMe)Me

Fmoc-Leu-Gln(Me)$_2$-N(OMe)Me (0.60 g, 1.09 mmol) in CH$_3$CN (6 ml) was treated with Et$_2$NH (5.6 ml) as above. To the N$^\alpha$-deprotected product in CH$_2$Cl$_2$–DMF (2.5 ml–2.5 ml), were added Fmoc-Val-OH (0.44 g, 1.30 mmol), BOP (0.58 g, 1.30 mmol), and DIEA (0.41 ml, 2.58 mmol). The mixture was stirred at 25 °C for 8 h and the crude product isolated as above was purified by silica-gel column chromatography using CHCl$_3$:MeOH–10:0.5 to yield the desired product as an oil. Yield 0.61 g (86%), [α]$_D^{27}$ −11.6 (c 1.0, CHCl$_3$), ^{1}H NMR (CDCl$_3$) δ; 0.86 (m, 12H), 1.49–1.65 (m, 2H), 1.97 (br s, 1H), 2.12–2.17 (m, 2H), 2.37–2.39 (m, 2H), 2.92 (s, 3H), 2.94 (s, 3H), 3.19 (s, 3H), 3.76 (s, 3H), 4.03 (br t, J = 7.2 Hz, 1H), 4.21 (t, J = 6.9 Hz, 1H), 4.31–4.53 (m, 3H), 4.92 (br s, 1H), 5.58 (br d, J = 8.7 Hz, 1H), 6.56 (br d, J = 7.5 Hz, 1 H), 7.30 (t, J = 7.5 Hz, 2H), 7.39 (t, J = 7.5 Hz, 2H), 7.59 (d, J = 7.5 Hz, 2H), 7.75 (d, J = 7.5 Hz, 2H); ^{13}C NMR δ; 17.97, 19.38, 22.10, 23.03, 24.83, 29.20, 31.25, 35.73, 37.28, 41.79, 47.32, 49.56, 52.01, 60.61, 61.71, 67.24, 120.08, 125.22, 127.21, 127.84, 141.43, 144.05, 156.58, 171.32, 171.85, 172.36; MALDI-TOF-MS; Calcd. 674.353 for C$_{35}$H$_{49}$N$_5$O$_7$Na, Found. 674.211 for [M+Na]$^+$.

3.6.4. Fmoc-Ala-Val-Leu-Gln(Me)$_2$-N(OMe)Me

Fmoc-Val-Leu-Gln(Me)$_2$-N(OMe)Me (0.60 g, 0.92 mmol) in CH$_2$Cl$_2$–CH$_3$CN (3 ml–3 ml) was treated with Et$_2$NH (4.8 ml) as above. To the product in DMF (5 ml), were added Fmoc-Ala-OH (0.34 g, 1.09 mmol), BOP (0.49 g, 1.09 mmol), and DIEA (0.35 ml, 2.20 mmol). The mixture was stirred at 25 °C for 8 h and the crude product isolated as above was purified by silica-gel column chromatography using CHCl$_3$:MeOH = 10:0.5 to yield the desired product as an oil. Yield 0.51 g (77%), [α]$_D^{27}$ −30.3 (c 0.90, CHCl$_3$), ^{1}H NMR (CDCl$_3$) δ; 0.87 (d, J = 6.6 Hz, 6H), 0.93 (d, J = 6.6 Hz, 6H), 1.36 (d, J = 6.9 Hz, 3H), 1.51–1.67 (m, 3H), 1.95–2.14 (m, 3H), 2.33–2.38 (m, 2H), 2.88 (s, 6H), 3.17(s, 3H), 3.72 (s, 3H), 4.20 (t, J = 7.2 Hz, 1H), 4.28–4.41 (m, 2H), 4.46 (br s, 1H), 4.57 (br s, 1H), 4.83 (br s, 1H), 5.08 (br s, 1H), 6.21 (br s, 1H), 7.24 (t, J = 7.2 Hz, 2H), 7.37 (t, J = 7.4 Hz, 2H), 7.60 (d, J = 7.5 Hz, 2H), 7.74 (d, J = 7.5 Hz, 2H), 7.95 (br s, 1H); ^{13}C NMR δ; 18.66, 19.42, 22.65, 22.88, 25.04, 27.92, 29.34, 31.51, 32.33, 35.58, 37.20, 42.06, 47.27, 49.01, 50.59, 51.76, 58.92, 61.79, 67.19, 120.06, 125.32, 127.17, 127.81, 141.39, 144.05, 162.49, 171.03, 172.07, 172.94; MALDI-TOF-MS; Calcd. 745.390 for C$_{38}$H$_{54}$N$_6$O$_8$Na, Found. 745.199 for [M+Na]$^+$.

3.6.5. Fmoc-Ser(Bu^t)-Ala-Val-Leu-Gln(Me)$_2$-N(OMe)Me

Fmoc-Ala-Val-Leu-Gln(Me)$_2$-N(OMe)Me (0.56 g, 0.77 mmol) in CH$_2$Cl$_2$–CH$_3$CN (3 ml–3 ml) was treated with Et$_2$NH (4.0 ml) as above. To the product in DMF (5 ml), were added Fmoc-Ser(Bu^t)-OH (0.36 g, 0.94 mmol), BOP (0.41 g, 0.94 mmol), and DIEA (0.30 ml, 1.89 mmol). The mixture was stirred at 25 °C for 2 h and the crude product isolated as above was purified by silica-gel column chromatography using CHCl$_3$:MeOH = 10:0.5 to yield the desired product as an oil. Yield 0.58 g (86%), [α]$_D^{27}$ −22.8 (c 0.15, CHCl$_3$), ^{1}H NMR (CDCl$_3$) δ; 0.84–0.92 (m, 12H), 1.15 (s, 9H), 1.34 (d, J = 6.6 Hz, 3H), 1.55–1.63 (m, 3H), 1.89–1.99 (m, 1H), 2.07–2.17 (m, 2H), 2.36 (br s, 2H), 2.88 (s, 3H), 2.89 (s, 3H), 3.17

(s, 3H), 3.47 (t, J = 7.8 Hz, 1H), 3.71 (t, J = 7.8 Hz, 1H), 3.73 (s, 3H), 4.21 (t, J = 7.1 Hz, 1H), 4.29–4.50 (m, 4H), 4.83 (br s, 1H), 4.94 (br s, 1H), 5.09 (br s, 1H), 6.39 (br s, 1H), 7.26 (br t, J = 7.4 Hz, 2H), 7.37 (br t, J = 7.4 Hz, 2H), 7.62 (br d, J = 6.9 Hz, 2H), 7.74 (br d, J = 7.2 Hz, 2H), 7.83 (br s, 1H), 8.03 (br s, 1H); ^{13}C NMR δ; 18.51, 19.26, 22.36, 22.79, 24.95, 27.35, 27.90, 29.20, 31.57, 35.42, 37.09, 41.80, 47.15, 48.99, 51.67, 54.98, 58.70, 61.70, 62.20, 67.05, 119.89, 125.22, 127.02, 127.65, 141.26, 143.92, 162.34, 170.02, 171.00, 172.00; MALDI-TOF-MS; Calcd. 888.041 for C$_{45}$H$_{66}$N$_7$O$_{10}$Na, Found. 888.253 for [M+Na]$^+$.

3.6.6. Fmoc-Thr(Bu^t)-Ser(Bu^t)-Ala-Val-Leu-Gln(Me)$_2$-N(OMe)Me

Fmoc-Ser(Bu^t)-Ala-Val-Leu-Gln(Me)$_2$-N(OMe)Me (0.57 g, 0.66 mmol) in CH$_2$Cl$_2$–CH$_3$CN (3 ml–3 ml) was treated with Et$_2$NH (3.4 ml) as above. To the product in DMF (5 ml), were added Fmoc-Thr(Bu^t)-OH (0.33 g, 0.80 mmol), BOP (0.35 g, 0.80 mmol), and DIEA (0.25 ml, 1.57 mmol). The mixture was stirred at 25 °C for 1 h and H$_2$O was added. The resulting precipitate was washed with 5% citric acid, 5% NaHCO$_3$, and H$_2$O. The crude product was reprecipitated from DMF/Et$_2$O to yield the desired product as an amorphous solid. Yield 0.40 g (59%), [α]$_D^{27}$ −13.2 (c 0.68, CHCl$_3$), ^{1}H NMR (CDCl$_3$) δ; 0.93-0.95 (br s, 12H), 1.17 (s, 12H), 1.31 (s, 9H), 1.41 (br d, J = 6.0 Hz, 3H), 1.67 (br s, 3H), 1.93 (br s, 1H), 2.13 (br s, 1H), 2.38 (br s, 3H), 2.92 (s, 3H), 2.97 (s, 3H), 3.20 (s, 3H), 3.51 (br s, 1H), 3.77 (s, 3H), 3.87 (br d, J = 7.8 Hz, 1H), 4.22 (br s, 4H), 4.42 (br s, 4H), 4.96 (br s, 1H), 6.78–6.81 (m, 2H), 7.14–7.41 (m, 7H), 7.58 (br d, J = 5.7 Hz, 2H), 7.77 (br d, J = 6.3 Hz, 2H); ^{13}C NMR δ; 17.28, 17.35, 17.89, 19.33, 21.48, 23.24, 24.73, 27.45, 28.30, 29.08, 29.65, 35.51, 37.23, 40.50, 47.22, 49.11, 50.49, 51.89, 54.52, 59.07, 60.83, 61.58, 66.72, 67.19, 120.08, 124.98, 125.08, 127.12, 127.84, 141.39, 143.61, 143.75, 156.07, 162.36, 169.63, 171.05, 171.35, 171.94, 172.31; MALDI-TOF-MS; Calcd. 1045.252 for C$_{53}$H$_{81}$N$_8$O$_{12}$Na, Found. 1045.426 for [M+Na]$^+$.

3.6.7. Ac-Thr(Bu^t)-Ser(Bu^t)-Ala-Val-Leu-Gln(Me)$_2$-N(OMe)Me

Fmoc-Thr(Bu^t)-Ser(Bu^t)-Ala-Val-Leu-Gln(Me)$_2$-N(OMe)Me (78 mg, 75 µmol) in CH$_2$Cl$_2$–CH$_3$CN (1.5 ml–1.5 ml) was treated with Et$_2$NH (0.59 ml) as above. To the product in DMF (3 ml), were added Ac$_2$O (0.14 ml, 1.48 mmol) and DIEA (0.24 ml, 1.48 mmol). The mixture was stirred at 25 °C for 8 h and H$_2$O was added. The crude product was reprecipitated from DMF/Et$_2$O to yield the desired product as an amorphous solid. Yield 40 mg (63%), [α]$_D^{27}$ −17.5 (c 0.20, DMF), ^{1}H NMR (DMSO-d_6) δ; 0.80–0.88 (m, 12H), 1.04 (d, J = 6.3 Hz, 3H), 1.10 (s, 9H), 1.11 (d, J = 6.6 Hz, 3H), 1.17 (s, 9H), 1.36–1.46 (m, 2H), 1.53–1.60 (m, 1H), 1.63–1.83 (m, 2H), 1.91 (s, 3H), 1.97 (m, 1H), 2.30 (br t, J = 7.4 Hz, 2H), 2.80 (s, 3H), 2.90 (s, 3H), 3.10 (s, 3H), 3.41–3.46 (m, 1H), 3.51–3.59 (m, 1H), 3.70 (s, 3H), 3.87–3.90 (m, 1H), 4.10–4.15 (m, 1H), 4.30–4.39 (m, 4H), 4.71 (br s, 1H), 7.61–7.97 (m, 6H); ^{13}C NMR δ; 18.49, 18.92, 19.64, 21.94, 22.97, 23.54, 24.40, 27.57, 28.45, 30.75, 35.29, 37.01, 48.61, 53.60, 57.75, 58.10, 62.25, 67.50, 169.89, 170.98, 171.64, 172.23; MALDI-TOF-MS; Calcd. 865.538 for C$_{40}$H$_{74}$N$_8$O$_{11}$Na, Found. 865.476 for [M+Na]$^+$.

3.6.8. Ac-Thr-Ser-Ala-Val-Leu-NHCH(CH$_2$CH$_2$CON(CH$_3$)$_2$)-CHO

LiAlH$_4$ (30 mg) was added to Ac-Thr(Bu^t)-Ser(Bu^t)-Ala-Val-Leu-Gln(Me)$_2$-N(OMe)Me (30 mg, 36 µmol) in DMF–THF (1.5 ml–1.5 ml), and the mixture was stirred at 25 °C for 90 min. The mixture was filtered and the solvent was evaporated. The crude product was purified by HPLC [Cosmosil 5C18 (10 × 250 mm), 3.0 ml/min, CH$_3$CN (15–60%)/30 min]. The solvent of the desired peak (rt, 42.0 min) was removed by lyophilization to yield a white fluffy powder. Yield 5.2 mg (19%) ^{1}H NMR (CD$_3$CN containing D$_2$O) δ; 0.82–0.93 (m, 12H), 1.10–1.14 (m, 3H), 1.14 (s, 9H), 1.17 (s, 9H), 1.31–1.36 (m, 3H), 1.56–1.64 (m, 3H), 2.00 (s, 3H), 2.10–2.17 (m, 1H), 2.28–2.33 (m, 2H), 2.85 (br s, 3H), 2.97 (br s, 3H), 3.61–3.70 (m, 2H), 3.97–4.02 (m, 1H), 4.10–4.24 (m, 6H), 9.41 (br s); MALDI-

TOF-MS; Calcd. 806.501 for $C_{38}H_{69}N_7O_{10}Na$, Found. 806.121 for $[M+Na]^+$.

Anisole (15 µl, 6.0 mmol) and TFA (0.5 ml) were added to the above powder (7.1 mg, 9 µmol), and the mixture was stirred at 25 °C for 2 h. The TFA was evaporated and ether (5 ml) and 0.1% aq.T-FA (5 ml) were added to the residue. The aqueous phase was washed with ether (5 ml) twice and the solvent was removed by lyophilization. The crude product was purified by HPLC [Cosmosil 5C18 (10 × 250 mm), 3.0 ml/min, CH$_3$CN (10–40%)/30 min]. The solvent of the desired peak (rt, 25.6 min) was removed by lyophilization to yield a white fluffy powder. Yield 1.8 mg (30%), HPLC rt, 14.36 min [Cosmosil 5C18 (4.6 × 150 mm), 1 ml/min, CH$_3$CN (10–40%)/30 min], ^{1}H NMR (CD$_3$CN containing D$_2$O) δ; 0.84–0.94 (m, 12H), 1.14–1.17 (m, 3H), 1.33–1.37 (m, 3H), 1.56–1.63 (m, 3H), 2.02 (s, 3H), 2.02–2.09 (m, 1H), 2.32–2.35 (m, 2H), 2.84–2.87 (m, 3H), 2.94–2.99 (m, 3H), 3.74–3.76 (m, 1H), 3.81–3.85 (m, 1H), 4.17–4.33 (m, 6H), 4.77–4.82 (m, 1H), 9.44 (br s); MALDI-TOF-MS; Calcd. 694.375 for $C_{30}H_{53}N_7O_{10}Na$, Found. 694.337 for $[M+Na]^+$.

The following truncated peptide-aldehyde derivatives were similarly prepared from the above intermediates.

3.6.9. Ac-Val-Leu-NHCH(CH$_2$CH$_2$CON(CH$_3$)$_2$)-CHO

HPLC rt, 18.64 min [Cosmosil 5C18 (4.6 × 150 mm), 1 ml/min, CH$_3$CN (10–60%)/30 min], ^{1}H NMR (CD$_3$CN) δ; 0.86–0.99 (m, 12 H), 1.51–1.64 (m, 3H), 2.03 (s, 3H), 2.31–2.37 (m, 2H), 3.98 (br t, J = 5.9 Hz, 1H), 4.27–4.33 (m, 1H), 4.55–4.63 (m, 1H), 4.78–4.86 (m, 1H), 6.82 (br d, J = 7.8 Hz, 2H), 6.96 (br d, J = 8.7 Hz, 1H), 9.42 (br s); MALDI-TOF-MS; Calcd. 435.259 for $C_{20}H_{46}N_4O_5Na$, Found. 435.955 for $[M+Na]^+$.

3.6.10. Ac-Ala-Val-Leu-NHCH(CH$_2$CH$_2$CON(CH$_3$)$_2$)-CHO

HPLC rt, 12.64 min [Cosmosil 5C18 (4.6 × 150 mm), 1 ml/min, CH$_3$CN (10–60%)/30 min], ^{1}H NMR (D$_2$O) δ; 0.86–0.94 (m, 12H), 1.33 (d, J = 7.2 Hz, 3H), 1.57–1.67 (m, 3H), 2.00 (s, 3H), 2.00–2.22 (m, 3H), 2.45–2.49 (m, 2H), 2.92 (s, 3H), 3.04 (s, 3H), 4.08 (d, J = 8.1 Hz, 1H), 4.28 (q, J = 7.2 Hz, 1H), 4.38–4.42 (m, 2H), 9.41 (br s); MALDI-TOF-MS; Calcd. 506.296 for $C_{23}H_{41}N_5O_6Na$, Found. 506.216 for $[M+Na]^+$.

3.6.11. Ac-Ser-Ala-Val-Leu-NHCH(CH$_2$CH$_2$CON(CH$_3$)$_2$)-CHO

HPLC rt, 14.38 min [Cosmosil 5C18 (4.6 × 150 mm), 1 ml/min, CH$_3$CN (10–40%)/30 min], ^{1}H NMR (CD$_3$CN containing D$_2$O) δ; 0.85–0.92 (m, 12H), 1.36 (d, J = 7.5 Hz, 3H), 1.56–1.66 (m, 3H), 1.98 (s, 3H), 2.07–2.10 (m, 1H), 2.30–2.35 (m, 2H), 2.86 (s, 3H), 2.99 (s, 3H), 3.64–3.69 (m, 1H), 3.77–3.83 (m, 1H), 4.00–4.02 (m, 1H), 4.19–4.30 (m, 23H), 9.44 (br s); MALDI-TOF-MS; Calcd. 593.328 for $C_{26}H_{46}N_6O_8Na$, Found. 593.258 for $[M+Na]^+$.

3.6.12. Ac-Ser-Ala-Val-Leu-Gln-NHCH$_3$

Ac-Ser(Bu^t)-Ala-Val-Leu-Gln(Trt)-N(OMe)Me was prepared similarly as above starting from Fmoc-Gln(Trt)-N(OMe)Me. The protected pentapeptide Weinreb amide (0.20 g, 0.22 mmol) in DMF (10 ml) was treated with LiAlH$_4$ as stated above. The products were absorbed on Diaion HP20 and eluted with CH$_3$CN:H$_2$O = 3:1. The solvent was removed by lyophilization, and the product was partially purified by HPLC [Cosmosil 5C18 (10 × 250 mm), 3 ml/min, CH$_3$CN (40–80%)/60 min]. An aliquot of the product was treated with TFA as stated above and purified by HPLC [Cosmosil 5C18 (10 × 250 mm), 3 ml/min, CH$_3$CN (10–40%)/60 min]. HPLC rt, 10.95 min [Cosmosil 5C18 (4.6 × 150 mm), 1 ml/min, CH$_3$CN (10–70%)/30 min], ^{1}H NMR (DMSO-d_6) δ; 0.81–0.91 (m, 12H), 1.21 (d, J = 7.2 Hz, 3H), 1.44–1.49 (m, 2H), 1.52–1.73 (m, 2H), 1.86 (s, 3H), 1.89–2.06 (m, 4H), 2.57 (d, J = 4.5 Hz, 3H), 3.52–3.55 (m, 2H), 4.07–4.33 (m, 4H), 4.98 (br t, J = 5.1 Hz, 1H), 7.69–7.73 (m, 2H), 7.94–8.14 (m, 4H); MALDI-TOF-MS; Calcd. 594.323 for $C_{25}H_{45}N_7O_8$-Na, Found. 594.268 for $[M+Na]^+$.

3.7. Inhibitory activity

Inhibitory activity was examined using the substrate SO1. Cleavage of the substrate by the purified mutant 3CL protease in the presence of various concentrations of the inhibitor was monitored by analytical HPLC, as described above. Inhibitory activity was evaluated using the corresponding IC$_{50}$ value obtained from the sigmoid dose-response curve. Reactions were repeated three times and the results were averaged.

References and notes

1. Lee, N.; Hui, D.; Wu, A.; Chan, P.; Cameron, P.; Joynt, F. M.; Ahuja, A.; Yung, M. Y.; Leung, C. B.; To, K. F.; Szeto, M. D.; Leu, C. C.; Chung, S.; Sung, J. J. Y. *N. Engl. J. Med.* **2003**, *348*, 1986–1994.
2. Drosten, C.; Günther, S.; Preiser, W.; Ven der Werf, S.; Brodt, H. R.; Becker, S.; Rabenau, H.; Panning, M.; Kolensnikova, L.; Fouchier, R. A. M.; Berger, A.; Burguière, A. M.; Cinatl, J.; Eickmann, M.; Escriou, N.; Grywna, K.; Kramme, S.; Manuguerra, J.; Müller, S.; Rickerts, V.; Stürmer, M.; Vieth, S.; Klenk, H. D.; Osterhaus, A. D. M. E.; Schmitz, H.; Doerr, H. W. *N. Engl. J. Med.* **2003**, *348*, 1967–1976.
3. Ksiazek, T. G.; Erdman, D.; Goldsmith, C. S.; Zaki, S. R.; Peret, T.; Emery, S.; Tong, S.; Urbani, C.; Comer, J. A.; Lim, W.; Rollin, P. E.; Dowell, S. F.; Ling, A. E.; Humphrey, C. D.; Shieh, W. J.; Guarner, J.; Paddock, C. D.; Rota, P.; Fields, B.; DeRisi, J.; Yang, J. Y.; Cox, N.; Hughes, J. M.; LeDuc, J. W.; Bellini, W. J.; Anderson, L. J. *N. Engl. J. Med.* **2003**, *348*, 1953–1966.
4. Rota, P. A.; Oberste, M. S.; Monroe, S. S.; Nix, W. A.; Campagnoli, R.; Icenogle, J. P.; Penaranda, S.; Bankamp, B.; Maher, K.; Chem, M. H.; Tong, W.; Tamin, A.; Lowe, L.; Frace, M.; DeRisi, J. L.; Chen, Q.; Wang, D.; Erdman, D. D.; Peret, T. C.; Burns, C.; Ksiazek, T. G.; Rollin, P. E.; Sanchez, A.; Liffick, S.; Holloway, B.; Limor, J.; McCaustland, K.; Olsen-Rasmussen, M.; Fouchier, R.; Gunther, S.; Osterhaus, A. D.; Drosten, C.; Pallansch, M. A.; Anderson, L. J.; Bellini, W. J. *Science* **2003**, *300*, 1394–1399.
5. Marra, M. A.; Jones, S. J.; Astell, C. R.; Holt, R. A.; Brooks-Wilson, A.; Butterfield, Y. S.; Khattra, J.; Asano, J. K.; Barber, S. A.; Chan, S. Y.; Cloutier, A.; Coughlin, S. M.; Freeman, D.; Girn, N.; Griffith, O. L.; Leach, S. R.; Mayo, M.; McDonald, H.; Montgomery, S. B.; Pandoh, P. K.; Petrescu, A. S.; Robertson, A. G.; Schein, J. E.; Siddiqui, A.; Smailus, D. E.; Sott, J. M.; Yang, G. S.; Plummer, F.; Andonov, A.; Artsob, H.; Bastien, N.; Bermard, K.; Booth, T. F.; Bowness, D.; Czub, M.; Drebot, M.; Fernando, L.; Flick, R.; Garbutt, M.; Gray, M.; Grolla, A.; Jones, S.; Feldmann, H.; Meyers, A.; Kabani, A.; Li, Y.; Normand, S.; Stroher, U.; Tipples, G. A.; Tyler, S.; Vogrig, R.; Ward, D.; Watson, B.; Brunham, R. C.; Krajden, M.; Petric, M.; Skowronski, D. M.; Upton, C.; Roper, R. L. *Science* **2003**, *300*, 1399–1404.
6. Thiel, V.; Ivanov, K. A.; Putics, Á.; Hertzig, T.; Schelle, B.; Bayer, S.; Weißbrich, B.; Snijder, E. J.; Rabenau, H.; Doerr, H. W.; Gorbalenya, A. E.; Ziebuhr, J. *J. Gen. Viol.* **2003**, *84*, 2305–2315.
7. Anand, K.; Palm, G. J.; Mesters, J. R.; Siddell, S. G.; Ziebuhr, J.; Hilgenfeld, R. *EMBO J.* **2002**, *21*, 3213–3224.
8. Anand, K.; Ziebuhr, J.; Wadhwani, P.; Mesters, J. R.; Hilgenfeld, R. *Science* **2003**, *300*, 1763–1767.
9. Fan, K.; Wei, P.; Feng, Q.; Chen, S.; Huang, C.; Ma, L.; Lai, B.; Pei, J.; Liu, Y.; Chen, J.; Lai, L. *J. Biol. Chem.* **2004**, *279*, 1637–1642.
10. Huang, C.; Wei, P.; Fan, K.; Liu, Y.; Lai, L. *Biochemistry* **2004**, *43*, 4568–4574.
11. Kaeppler, U.; Stiefl, N.; Schiller, M.; Vicik, R.; Breuning, A.; Schmitz, W.; Rupprecht, D.; Schmuck, C.; Baumann, K.; Ziebuhr, J.; Schirmeister, T. *J. Med. Chem.* **2005**, *48*, 6832–6842.
12. Ghosh, A. K.; Xi, K.; Ratia, K.; Santarsiero, B. D.; Fu, W.; Harcourt, B. H.; Rota, P. A.; Baker, S. C.; Johnson, M. E.; Mesecar, A. D. *J. Med. Chem.* **2005**, *48*, 6767–6771.
13. Shie, J. J.; Fang, J. M.; Kuo, C. J.; Kuo, T. H.; Liang, P. H.; Huang, H. J.; Yang, W. W.; Lin, C. H.; Chen, J. L.; Wu, Y. T.; Wong, C. H. *J. Med. Chem.* **2005**, *48*, 4469–4473.
14. Chen, L. R.; Wang, Y. C.; Lin, Y. W.; Chou, S. Y.; Chen, S. F.; Liu, L. T.; Wu, Y. T.; Kuo, C. J.; Chen, T. S. S.; Juang, S. H. *Bioorg. Med. Chem. Lett.* **2005**, *15*, 3058–3062.
15. Shie, J. J.; Fang, J. M.; Kuo, T. H.; Kuo, C. J.; Liang, P. H.; Huang, H. J.; Wu, Y. T.; Jan, J. T.; Cheng, Y. S.; Wong, C. H. *Bioorg. Med. Chem.* **2005**, *13*, 5240–5252.
16. Jain, R. P.; Petterson, H. I.; Zhang, J.; Aull, K. D.; Fortin, P. D.; Huitema, C.; Eltis, L. D.; Parrish, J. C.; James, M. N. G.; Wishart, D. S.; Vederas, J. C. *J. Med. Chem.* **2004**, *47*, 6113–6116.
17. Ghosh, A. K.; Xi, K.; Grum-Tokars, V.; Xu, X.; Ratia, K.; Fu, W.; Houser, K. V.; Baker, S. C.; Johnson, M. E.; Mesecar, A. D. *Bioorg. Med. Chem. Lett.* **2007**, *17*, 5876–5880.
18. Bacha, U.; Barrila, J.; Velazquez-Campoy, A.; Leavitt, S. A.; Freire, E. *Biochemistry* **2004**, *43*, 4906–4912.

19. Chou, C. Y.; Chang, H. C.; Hsu, W. C.; Lin, T. Z.; Lin, C. H.; Chang, G. G. *Biochemistry* **2004**, *43*, 14958–14970.
20. Lee, T. W.; Cherney, M. M.; Huitema, C.; Liu, J.; James, K. E.; Powers, J. C.; Eltis, L. D.; James, M. N. G. *J. Mol. Biol.* **2005**, *353*, 1137–1151.
21. Yang, S.; Chen, S. J.; Hsu, M. F.; Wu, J. D.; Tseng, C. T. K.; Liu, Y. F.; Chen, H. C.; Kuo, C. W.; Wu, C. S.; Chang, L. W.; Chen, W. C.; Liao, S. Y.; Chang, T. Y.; Hung, H. H.; Shr, H. L.; Liu, C. Y.; Huang, Y. A.; Chang, L. Y.; Hsu, J. C.; Peters, C. J.; Wang, A. H. J.; Hsu, M. C. *J. Med. Chem.* **2006**, *49*, 4971–4980.
22. Al-Gharabli, S.; AliShah, S. T.; Weik, S.; Schmidt, M. F.; Mesters, J. R.; Kuhn, D.; Klebe, G.; Hilgenfeld, R.; Rademann, J. *ChemBioChem* **2006**, *7*, 1048–1055.
23. Yang, H.; Yang, M.; Ding, Y.; Liu, Y.; Lou, Z.; Zhou, Z.; Sun, L.; Mo, L.; Ye, S.; Pang, H.; Gao, G. F.; Anand, K.; Bartlam, M.; Hilgenfeld, R.; Rao, Z. *Proc. Natl. Acad. Sci. U.S.A.* **2003**, *100*, 13190–13195.
24. Hsu, M. F.; Kuo, C. J.; Chang, K. T.; Chang, H. C.; Chou, C. C.; Ko, T. P.; Shr, H. L.; Chang, G. G.; Wang, A. H. J.; Liang, P. H. *J. Biol. Chem.* **2005**, *280*, 31257–31266.
25. Nahm, S.; Weinreb, S. M. *Tetrahedron Lett.* **1981**, *22*, 3815–3818.
26. Sydnes, M. O.; Hayashi, Y.; Sharma, V. K.; Hamada, T.; Bacha, U.; Barrila, J.; Freire, E.; Kiso, Y. *Tetrahedron* **2006**, *62*, 8601–8609.
27. Hanada, K.; Tamai, M.; Yamagishi, M.; Ohmura, S.; Sawada, J.; Tanaka, I. *Agric. Biol. Chem.* **1978**, *42*, 523–528.
28. Matsudaira, P. *J. Biol. Chem.* **1987**, *262*, 10035–10038.
29. Stemmer, W. P. C.; Morris, S. K. *BioTechniques* **1992**, *13*, 214–220.
30. Atherton, E.; Wellings, D. In *Synthesis of Peptides and Peptidemimetics E22a*; Goodman, M., Ed.; Georg Thieme Verlag: Stuttgart, 2004; pp 740–754.
31. Rink, H. *Tetrahedron Lett.* **1987**, *28*, 3787–3790.